

completion of the three viscous load conditions (Supplementary Information). Monkey C was trained to perform movements with loads to eight directions uniformly distributed in hand-space. In order to save time during the viscous load conditions, neural activity was recorded only to targets at 90° and 270°, directions associated with large shoulder and elbow rotations, and thus large loads (Supplementary Information).

**Data analysis**

Cell activity was represented as the number of action potentials recorded between 150 ms before movement onset (defined on the basis of 5% of peak tangential hand velocity) and peak tangential hand velocity. Muscle torques at the shoulder and elbow were computed using inverse dynamics<sup>9</sup>. Differences in mean cell discharge were assessed between load conditions and across movement directions using two-way ANOVA followed by individual comparisons between means using a Bonferroni correction for multiple comparisons. For monkeys A and B, differences were considered significant at  $P < 0.0021$  ( $P < 0.05 / 24$  comparisons: 8 target directions  $\times$  3 load conditions); for monkey C differences were considered significant at  $P < 0.0083$  ( $P < 0.05 / 6$  comparisons: 2 targets  $\times$  3 loads). All probability values reported in the text represent Bonferroni-corrected values.

The preferred direction (PD), the direction of maximal activity, of each cell for unloaded reaching movements was computed<sup>10,21</sup>. We also defined a load-related PD based on the absolute change in cell activity between NL and each load condition. In this case, the preferred direction signified the largest change (either increase or decrease) in activity. Bootstrap techniques were used to identify whether these directional signals were statistically significant ( $P < 0.01$ )<sup>10,20</sup>.

In each monkey, the EMG activity of up to 16 forelimb muscles (mono- and bi-articular muscles spanning shoulder and elbow) was recorded during conditions NL, VB, VS and VE. Pairs of single-strand wires were inserted percutaneously in monkeys A, B and C, and pairs of multi-strand wires were implanted chronically in monkeys A and C under aseptic conditions<sup>10,22</sup>. Some muscles were sampled twice in monkeys A and C, once using chronically implanted wires and a second time using percutaneously inserted wires providing a total of 57 samples of EMG (Supplementary Information).

Received 25 January; accepted 16 April 2002; doi:10.1038/nature00834.

1. Wolpert, D. M. & Ghahramani, Z. Computational principles of movement neuroscience. *Nature Neurosci.* **3** suppl., 1212–1217 (2000).
2. Wolpert, D. M. & Kawato, M. Multiple paired forward and inverse models for motor control. *Neural Netw.* **11**, 1317–1329 (1998).
3. Shadmehr, R. & Mussa-Ivaldi, F. A. Adaptive representation of dynamics during learning of a motor task. *J. Neurosci.* **14**, 3208–3224 (1994).
4. Kalaska, J. F., Cohen, D. A., Hyde, M. L. & Prud'homme, M. A comparison of movement direction-related versus load direction-related activity in primate motor cortex, using a two-dimensional reaching task. *J. Neurosci.* **9**, 2080–2102 (1989).
5. Gandolfo, F., Li, C., Benda, B. J., Schioppa, C. P. & Bizzi, E. Cortical correlates of learning in monkeys adapting to a new dynamical environment. *Proc. Natl Acad. Sci. USA* **97**, 2259–2263 (2000).
6. Kalaska, J. F., Scott, S. H., Cisek, P. & Sergio, L. E. Cortical control of reaching movements. *Curr. Opin. Neurobiol.* **7**, 849–859 (1997).
7. Porter, R. & Lemon, R. *Corticospinal Function and Voluntary Movement* (Oxford Univ. Press, Oxford, 1995).
8. Ashe, J. Force and the motor cortex. *Behav. Brain Res.* **87**, 255–269 (1997).
9. Scott, S. H. Apparatus for measuring and perturbing shoulder and elbow joint positions and torques during reaching. *J. Neurosci. Methods* **89**, 119–127 (1999).
10. Scott, S. H., Gribble, P. L., Graham, K. M. & Cabel, D. W. Dissociation between hand motion and population vectors from neural activity in motor cortex. *Nature* **413**, 161–165 (2001).
11. Humphrey, D. R. & Reed, D. J. in *Motor Control Mechanisms in Health and Disease* Advances in Neurology no. 39 (ed. Desmedt, J.) 347–372 (Raven, New York, 1983).
12. Fetz, E. E., Cheney, P. D., Mewes, K. & Palmer, S. in *Peripheral Control of Posture and Locomotion* (eds Allum, J. A. H. & Hulliger, M.) 437–449 (Elsevier, New York, 1989).
13. Cabel, D. W., Cisek, P. & Scott, S. H. Neural activity in primary motor cortex related to mechanical loads applied to the shoulder and elbow during a postural task. *J. Neurophysiol.* **86**, 2102–2108 (2001).
14. Sanes, J. N. & Schieber, M. H. Orderly somatotopy in primary motor cortex: does it exist? *Neuroimage* **13**, 968–974 (2001).
15. McKiernan, B. J., Marcario, J. K., Karrer, J. H. & Cheney, P. D. Corticomotorneural postspike effects in shoulder, elbow, wrist, digit, and intrinsic hand muscles during a reach and prehension task. *J. Neurophysiol.* **80**, 1961–1980 (1998).
16. Imamizu, H. et al. Human cerebellar activity reflecting an acquired internal model of a new tool. *Nature* **403**, 192–195 (2000).
17. Wolpert, D. M., Miall, R. C. & Kawato, M. Internal models in the cerebellum. *Trends Cogn. Sci.* **2**, 338–347 (1998).
18. Schmidt, R. A. & Wrisbert, C. A. *Motor Learning and Performance: A Problem-Based Learning Approach* (Human Kinetics, Champaign, 2000).
19. Wightman, D. C. & Lintern, G. Part-task training for tracking and manual control. *Hum. Factors* **27**, 267–283 (1985).
20. Scott, S. H. & Kalaska, J. F. Reaching movements with similar hand paths but different arm orientations. I. Activity of individual cells in motor cortex. *J. Neurophysiol.* **77**, 826–852 (1997).
21. Gribble, P. L. & Scott, S. H. Method for assessing directional characteristics of non-uniformly sampled neural activity. *J. Neurosci. Methods* **113**, 187–197 (2002).
22. Loeb, G. E. & Gans, C. *Electromyography for Experimentalists* (Univ. Chicago Press, Chicago, 1986).

Supplementary Information accompanies the paper on Nature's website (<http://www.nature.com/nature>).

**Acknowledgements**

We thank K. Moore for technical assistance, and D.W. Cabel and S. Chan who assisted in some of the training and neuronal recording sessions. We thank D. Munoz, M. Pare and K. Rose for comments on this manuscript. This work was supported by a CIHR grant and scholarship (S.H.S.) and a CIHR postdoctoral fellowship (P.L.G.).

**Competing interests statement**

The authors declare competing financial interests: details accompany the paper on Nature's website (<http://www.nature.com>).

Correspondence and requests for materials should be addressed to S.H.S. (e-mail: [steve@biomed.queensu.ca](mailto:steve@biomed.queensu.ca)).

**Oligodendrocyte-myelin glycoprotein is a Nogo receptor ligand that inhibits neurite outgrowth**

Kevin C. Wang\*†, Vuk Koprivica\*†, Jieun A. Kim\*, Rajeev Sivasankaran\*, Yong Guo‡, Rachel L. Neve†§ & Zhigang He\*†

\* Division of Neuroscience, Children's Hospital, and † Program in Neuroscience, Harvard Medical School, 320 Longwood Avenue, Boston, Massachusetts 02115, USA

‡ Aventis Pharmaceuticals, Bridgewater, New Jersey 08807, USA

§ McLean Hospital, 115 Mill Street, Belmont, Massachusetts 02478, USA

The inhibitory activity associated with myelin is a major obstacle for successful axon regeneration in the adult mammalian central nervous system (CNS)<sup>1,2</sup>. In addition to myelin-associated glycoprotein (MAG)<sup>3,4</sup> and Nogo-A<sup>5–7</sup>, available evidence suggests the existence of additional inhibitors in CNS myelin<sup>8</sup>. We show here that a glycosylphosphatidylinositol (GPI)-anchored CNS myelin protein, oligodendrocyte-myelin glycoprotein (OMgp), is a potent inhibitor of neurite outgrowth in cultured neurons. Like Nogo-A, OMgp contributes significantly to the inhibitory activity associated with CNS myelin. To further elucidate the mechanisms that mediate this inhibitory activity of OMgp, we screened an expression library and identified the Nogo receptor (NgR)<sup>9</sup> as a high-affinity OMgp-binding protein. Cleavage of NgR and other GPI-linked proteins from the cell surface renders axons of dorsal root ganglia insensitive to OMgp. Introduction of exogenous NgR confers OMgp responsiveness to otherwise insensitive neurons. Thus, OMgp is an important inhibitor of neurite outgrowth that acts through NgR and its associated receptor complex. Interfering with the OMgp/NgR pathway may allow lesioned axons to regenerate after injury *in vivo*.

To examine whether any GPI-linked proteins in CNS myelin act as inhibitors of neurite outgrowth, we treated purified myelin from bovine white matter with phosphatidylinositol-specific phospholipase C (PI-PLC) and examined the released proteins for their ability to alter growth cone morphology in an assay of growth cone collapse using dorsal root ganglia from chicks at embryonic day 13 (E13 DRG)<sup>6,9,10</sup>. PI-PLC-released proteins from CNS myelin exhibited marked growth cone collapsing activity (Fig. 1). By SDS-polyacrylamide gel electrophoresis (PAGE) and silver staining, we found that a band of relative molecular mass about 110,000 ( $M_r \sim 110K$ ) was significantly enriched in this fraction (Fig. 2a). Because the size of this band was similar to that of a previously identified CNS myelin protein, OMgp<sup>11,12</sup>, we used anti-OMgp antibodies to detect enrichment of cleaved OMgp in the PI-PLC supernatants by western blot. Anti-OMgp antibodies detected a band of comparable size in the PI-PLC-treated supernatants

(Fig. 2b), suggesting that OMgp is a component released from CNS myelin by PI-PLC. Next, we examined whether purified recombinant OMgp protein was able to inhibit neurite outgrowth in both the growth cone collapse<sup>6,9,13</sup> and the neurite outgrowth assays<sup>3-7,9</sup>. Like the PI-PLC-treated myelin supernatants, purified recombinant polyhistidine-tagged OMgp protein (OM-His), but not proteins purified from COS-7 cells transfected with a control vector (data not shown), induced the collapse of E13 DRG growth cones dose dependently. The effective concentration for half-maximal response (EC<sub>50</sub>) for OM-His was about 1.5 nM (Fig. 2c). Consistent with the notion that it is an inhibitor of neurite outgrowth, the OMgp protein is highly expressed by mature oligodendrocytes positive for myelin basic protein (MBP)<sup>14</sup>, and enriched in the axon-adjacent myelin layers<sup>11,12</sup>. Moreover, OM-His, when presented either as an immobilized substrate or in a soluble form (Fig. 2d, e), inhibited neurite outgrowth of cerebellar granule neurons (CGNs) from rats at postnatal day 7-9 (P7-9), also dose dependently. The OMgp-induced inhibitory responses were similar to that brought about by treatment of the same neurons with an alkaline phosphatase fusion protein containing the 66-amino-acid extracellular domain of Nogo-A (AP-66)<sup>6,9</sup> (Fig. 2c-e). This suggests that OMgp, like Nogo-66, is a potent neurite outgrowth inhibitor.

To further examine the functional importance of OMgp as a CNS myelin-associated inhibitor, we used peanut agglutinin (PNA)-agarose beads<sup>11</sup> to specifically deplete OMgp from solubilized CNS myelin. Although the inhibitory activity in the PNA-depleted myelin was significantly lower than that in control myelin, the OMgp-enriched eluates from the same PNA column displayed a potent inhibitory activity (see Supplementary Information). By using a combination of PNA-agarose<sup>11</sup> and Q-Sepharose<sup>3,15,16</sup> columns, we generated myelin fractions enriched in MAG, Nogo-A or OMgp. Comparisons of the EC<sub>50</sub> for each of these fractions show that the OMgp-enriched fraction inhibited neurite outgrowth to a similar extent as the Nogo-A-enriched fraction, but more than the MAG-enriched fraction (see Supplementary Information).

To investigate the mechanisms by which OMgp inhibits neurite outgrowth, we used an AP-OMgp fusion protein (AP-OM) as a probe to identify OMgp-binding proteins on the cell surface by an expression cloning strategy<sup>9,13,17</sup>. We examined pools of complementary DNA from an adult human brain cDNA expression

library, and isolated two cDNAs that encoded OMgp-binding proteins. Sequence analysis revealed that both cDNAs contained the full-length coding region of the Nogo-66 receptor (NgR), a high-affinity receptor for the extracellular domain of Nogo-A (ref. 9). We then determined the binding affinity of expressed NgR for AP-OM as 5 nM, similar to that determined for Nogo-66 (7 nM)<sup>9</sup>. These data suggest that NgR is a protein that binds OMgp with high affinity. We next performed co-precipitation experiments by incubating glutathione S-transferase (GST) or a GST fusion protein containing the entire extracellular domain of NgR (GST-NgR) with or without OM-His. GST-NgR (Fig. 3a, lane 6), but not

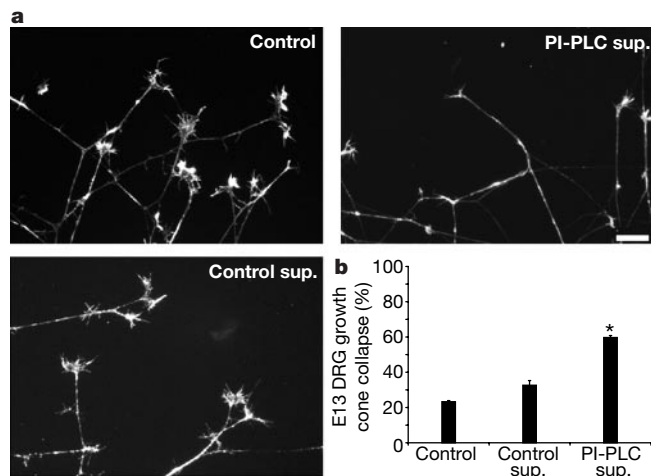


**Figure 1** GPI-anchored myelin component(s) induces growth cone collapse. **a**, Chick E13 DRG explants exposed to nothing (control), and the supernatant of CNS myelin-treated with (PI-PLC sup.) or without (control sup.) PI-PLC. Scale bar, 40  $\mu$ m. **b**, Quantification of the results shown in **a**. Asterisk, collapse significantly different ( $P < 0.005$ , Student's *t*-test) from control.

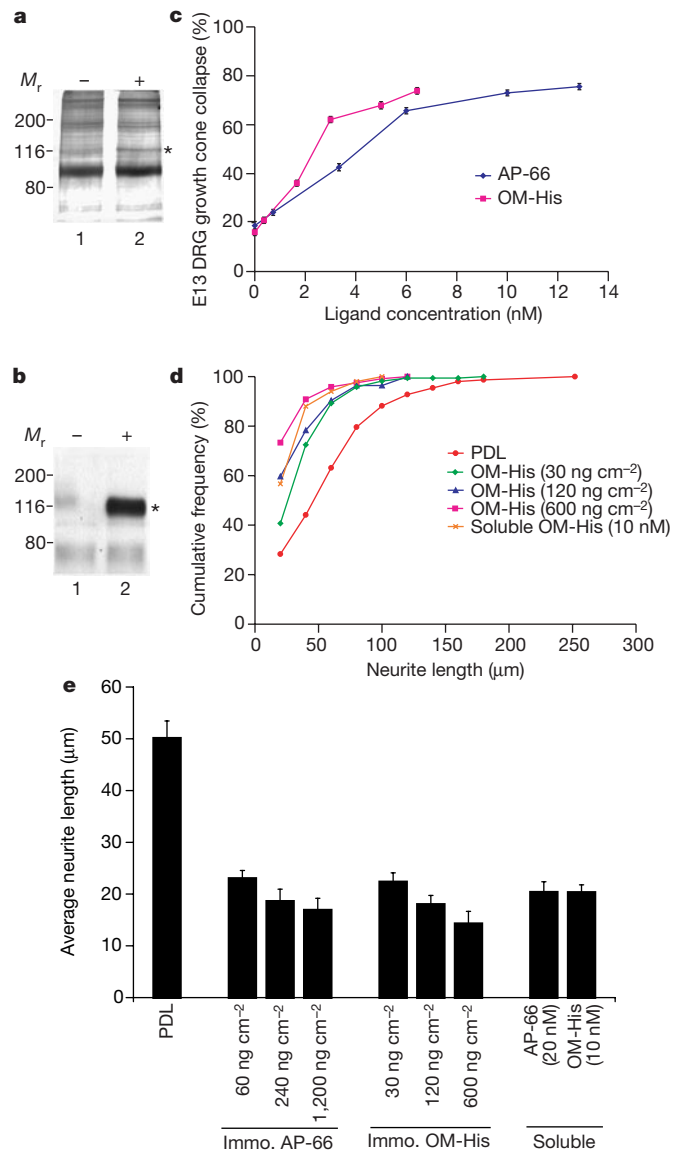


**Figure 2** OMgp is a myelin-associated inhibitor. **a**, Silver staining of untreated (-, lane 1) and PI-PLC-treated (+, lane 2) protein supernatants. **b**, Western blot of the same samples probed with anti-OMgp antibodies. **c**, Quantification of the results of E13 chick DRG growth cone collapse assays. Estimated EC<sub>50</sub>: 2.3 nM (AP-66) and 1.5 nM (OM-His). **d**, Distributions of rat CGNs with different neurite lengths plotted as cumulative histograms. **e**, Neurite lengths (mean  $\pm$  s.e.m.) quantified from neurons cultured on immobilized substrates or in the presence of soluble recombinant proteins. Statistical analysis was done by one-way analysis of variance (ANOVA) ( $F = 48.78$ , d.f. = 26,  $P < 0.001$ ) using a post-hoc Fisher protected test. All groups are significantly different from the control PDL group in **d** and **e**.

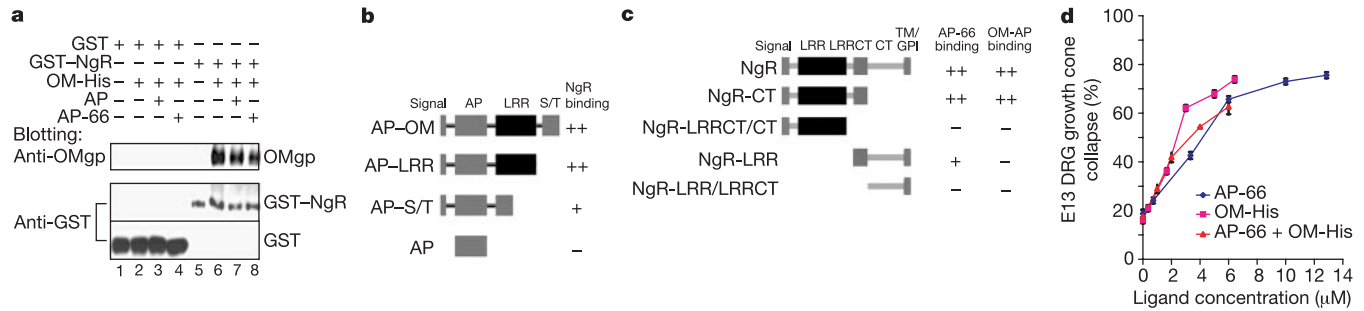


**Figure 3** The Nogo-66 receptor is an OMgp-binding protein. **a**, Co-precipitation of GST or GST-NgR with OM-His in the presence of AP or AP-66. **b**, Summary diagram of different AP-OMgp fusion proteins binding to NgR-expressing cells. Signal, signal peptide. **c**, Summary diagram of AP-66 and OM-AP binding to COS-7 cells expressing different

truncations of NgR. CT, unique C-terminal region; TM/GPI, transmembrane domain/GPI anchor. **d**, Growth cone collapse responses of E13 chick DRG induced by AP-66 alone, OM-His alone, or AP-66 plus OM-His (estimated EC<sub>50</sub> are 2.3 ± 1.3 nM, 1.6 ± 1.3 nM and 2.5 ± 1.1 nM for these treatments, respectively).

the control GST protein (lane 2), bound to OM-His, suggesting a direct interaction between NgR and OMgp. We further determined which domain(s) of OMgp was responsible for binding to NgR. Like NgR, OMgp is a GPI-linked protein containing a leucine-rich repeat (LRR) domain. An AP fusion protein containing only the LRR domain of OMgp (AP-LRR) was found to be sufficient to bind strongly to NgR-expressing cells (Fig. 3b). In addition, the carboxy-terminal domain with serine-threonine repeats (AP-S/T) alone was also able to bind weakly to NgR-expressing cells (Fig. 3b).

To explore how NgR interacts at the molecular level with these two inhibitors, we made a series of deletion constructs of NgR. We found that, although both the LRR and C-terminal LRR (LRRCT) domains of NgR were required for binding to OMgp, the LRRCT domain alone was sufficient for binding to Nogo-66 (Fig. 3c). Thus, OMgp and Nogo-66 bind to overlapping regions of NgR. In assays of cell-surface binding (data not shown) and co-precipitation (Fig. 3a), AP-66 and OM-His proteins consistently competed for binding to NgR. To examine the functional consequences of the molecular interaction of the two ligands with NgR, we compared the collapsing activity of OM-His plus AP-66 with that of OM-His or AP-66 alone (Fig. 3d). The estimated EC<sub>50</sub> for OM-His

plus AP-66 (2.5 nM) was similar to that for OM-His (1.5 nM) and AP-66 (2.3 nM), suggesting a redundant effect between OM-His and AP-66 in inducing growth cone collapse. Because the binding affinities of both OMgp and Nogo-66 to NgR are similar, our results imply that these two myelin components act independently through NgR to inhibit neurite outgrowth.

Because the GPI-linked NgR protein can be released by PI-PLC, we next examined whether PI-PLC treatment could affect axonal responsiveness to OMgp. Consistent with a previous study<sup>9</sup>, PI-PLC treatment did not alter the growth cone morphology of E13 chick DRG neurons, but rendered these axons insensitive to Nogo-66 (Fig. 4a). Similarly, PI-PLC treatment abolished the growth cone collapsing activity of OMgp (Fig. 4a). As a control, the growth cone collapsing activity of Semaphorin 3A<sup>10,13</sup>, known to be mediated by transmembrane receptor molecules including neuropilin-1 and members of the plexin family<sup>18</sup>, was not affected by PI-PLC treatment (Fig. 4a). Even though PI-PLC also cleaves other GPI-anchored proteins on the axonal surface, these results support the notion that GPI-anchored proteins, most probably NgR, act as necessary signal transducers of the inhibitory activity of OMgp.

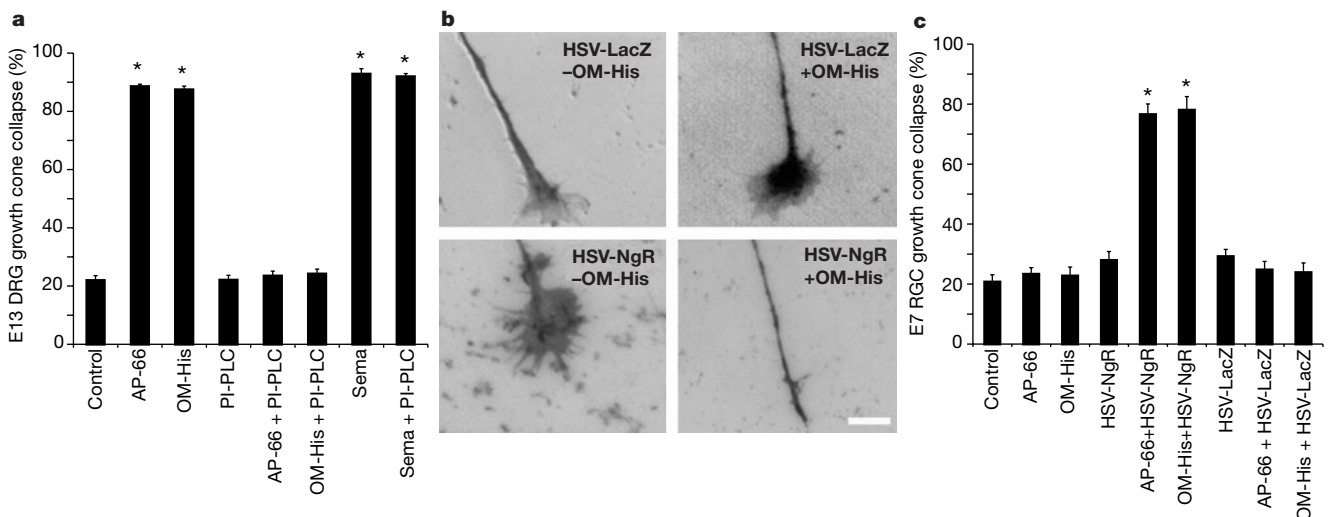


**Figure 4** NgR mediates OMgp-elicited growth cone collapse. **a**, Results of growth cone collapse assays on E13 chick DRG. Statistical analysis was by one-way ANOVA ( $F = 1,249$ , d.f. = 23,  $P < 0.0001$ ), using a post-hoc Fisher protected test. **b**, Collapse responses to OM-His of chick E7 RGC explants infected with HSV-LacZ or HSV-NgR. Scale

bar, 5 μm. **c**, Quantified results from **b**. Statistical analysis was by one-way ANOVA ( $F = 126.6$ , d.f. = 26,  $P < 0.0001$ ), using a post-hoc Fisher protected test. Asterisks in **a** and **c** mark collapse percentages significantly different from untreated controls.



To assess whether NgR is capable of mediating OMgp-induced inhibitory activity on neurite outgrowth, we took a gain-of-function approach to examine whether expression of NgR conferred OMgp responsiveness to otherwise insensitive neurons. Chick E7 retinal ganglion neurons (RGN) are insensitive to Nogo-66, but introduction of exogenous NgR in these neurons renders their growth cones responsive to Nogo-66 (ref. 9). Using the same strategy, we made a recombinant herpes simplex virus (HSV) that drives expression of a Flag-tagged full-length human NgR (Flag-NgR) in infected neurons. Upon infection, 80% of the E7 RGNs expressed the Flag-NgR protein, as assessed by immunocytochemistry with an anti-Flag antibody. No significant morphological changes were observed in the HSV-infected neurons (Fig. 4b, c). Consistent with a previous study<sup>9</sup>, expression of Flag-NgR, but not control  $\beta$ -galactosidase, conferred a growth cone collapse response to Nogo-66 in E7 RGN (Fig. 4c). Furthermore, the growth cones of NgR-expressing axons also became collapsible by OMgp (Fig. 4b, c). Taken together, our results suggest that, like Nogo-66, OMgp acts through NgR and its associated receptor complex to inhibit axon outgrowth. In contrast to Nogo-A, most of which is localized intracellularly<sup>5-7</sup>, OMgp is predominantly localized on the surfaces of oligodendrocytes and axon-adjacent myelin layers<sup>11,12,14</sup>, suggesting that OMgp is a physiological ligand of NgR. Although the precise contributions of OMgp and Nogo-A in restricting axon regeneration *in vivo* remain to be determined, our results suggest that multiple inhibitors may exert their effects through the same signalling pathway, which may provide crucial insights into stimulating axon regeneration after human CNS injury. □

## Methods

### Purification, PI-PLC treatment and OMgp depletion of myelin

Myelin was prepared from white matter of bovine brain according to established protocols<sup>19</sup>. For PI-PLC treatment, aliquots of myelin suspensions in water (10 mg ml<sup>-1</sup>) were incubated with or without 2.5 U ml<sup>-1</sup> PI-PLC (Sigma) at 37 °C for 2 h, before centrifugation (360,000g for 60 min). The supernatants were concentrated, partitioned in Triton X-114, and used for assays and for detection by western analysis.

### Expression cloning and binding experiments

Sequences encoding mouse OMgp were amplified from Marathon-ready mouse cDNA (Clontech) and confirmed by sequencing analysis, before subcloning into the expression vector AP-5 (ref. 9) to express an AP-OM fusion protein tagged with both a polyhistidine and a Myc epitope. The resultant plasmid DNA was transfected into COS-7 cells and the secreted protein purified using nickel-agarose resins (Qiagen).

For expression cloning of OMgp-binding proteins, pools of 5,000 arrayed clones from a human brain cDNA library (Origene Technologies) were transfected into COS-7 cells, and cell-surface binding with AP-OM was performed as described previously<sup>4,13,17</sup>. We isolated single NgR cDNA clones by subdividing the pools and sequencing analysis.

### Recombinant proteins and viruses and co-precipitation

To express recombinant OMgp for functional assays, we subcloned the coding region of mouse OMgp (amino acids 23–392) into pSecTag B (Invitrogen) to express His-tagged OMgp protein (OM-His) in COS-7 cells. The expressed OM-His protein was purified using a nickel resin. To construct recombinant HSV, cDNAs for Flag-tagged NgR or  $\beta$ -galactosidase were inserted into the HSV amplicon HSV-PrpUC and packaged into the virus using helper 5dl1.2, as described previously<sup>20</sup>. To produce recombinant Nogo-66 protein, the sequence of Nogo-66 was amplified from a human cDNA clone, KIAA0886 (Kazusa DNA Research Institute), and used to generate a construct expressing the AP-66 protein as described elsewhere<sup>6</sup>. Antibodies against Nogo-A and MAG were purchased from Alpha Diagnostics and R&D Systems, respectively.

In co-precipitation experiments, 2  $\mu$ g GST or GST-NgR were first immobilized to glutathione-agarose beads and the beads were further incubated with or without 1  $\mu$ g OM-His in the presence of 2  $\mu$ g of AP or AP-66 at 4 °C for 2 h. After extensive washing, bound proteins were resolved with SDS-PAGE and detected by western blotting.

### Growth cone collapse and neurite outgrowth assays

Chick E13 DRG and E7 retina were isolated and cultured as described previously<sup>9,10</sup>. DRG explants cultured overnight were used for growth cone collapse assays. In untreated control cultures, 80–85% of the growth cones were intact. To assess the effects of PI-PLC treatment, cultures were pre-incubated with 2 U ml<sup>-1</sup> PI-PLC for 30 min before treatment with individual test proteins for another 30 min. To express NgR in E7 retinal ganglion neurons, we infected the explants with recombinant HSV for 24 h. After incubation with each test protein for 30 min, retinal explants were fixed in 4% paraformaldehyde and 15% sucrose. Infection of HSV-LacZ was detected by a standard  $\beta$ -galactosidase staining protocol<sup>20</sup>. Flag-NgR expression was detected by incubating paraformaldehyde-fixed

cultures with the M2 anti-Flag antibody. Bound antibody was detected by incubation with AP-conjugated anti-rabbit immunoglobulin- $\gamma$  (IgG) secondary antibody and reaction with nitroblue tetrazolium (NBT) and 5-bromo-4-chloro-3-indoxyl phosphate (BCIP)<sup>22</sup>. Growth cone collapse was quantified only in those positively stained for  $\beta$ -galactosidase or immunoreactive for the Flag epitope. The means  $\pm$  s.e.m. from more than 400 growth cones per condition in three separate experiments are presented.

Neurite outgrowth assays were performed as described previously<sup>15,21</sup>. Briefly, P7–9 rat CGNs were dissected and then plated at a density of  $1 \times 10^5$  cells per well. Cells were cultured for 24 h before being fixed with 4% paraformaldehyde and stained with a neuronal-specific anti- $\beta$ -tubulin antibody (Tuj-1, Covance). Neurite lengths were measured from at least 150 CGNs per condition, from duplicate wells per experiment, and from three independent experiments, and quantified as described previously<sup>23</sup>.

Received 3 April; accepted 23 May 2002; doi:10.1038/nature00867.

Published online 16 June 2002.

- Schwab, M. E. & Bartholdi, D. Degeneration and regeneration of axons in the lesioned spinal cord. *Physiol. Rev.* **76**, 319–370 (1996).
- Horner, P. J. & Gage, F. H. Regenerating the damaged central nervous system. *Nature* **407**, 963–970 (2000).
- McKerracher, L. *et al.* Identification of myelin-associated glycoprotein as a major myelin-derived inhibitor of neurite growth. *Neuron* **13**, 805–811 (1994).
- Mukhopadhyay, G. *et al.* A novel role for myelin-associated glycoprotein as an inhibitor of axonal regeneration. *Neuron* **13**, 757–767 (1994).
- Chen, M. S. *et al.* Nogo-A is a myelin-associated neurite outgrowth inhibitor and an antigen for monoclonal antibody IN-1. *Nature* **403**, 434–439 (2000).
- GrandPre, T., Nakamura, F., Vartanian, T. & Strittmatter, S. M. Identification of the Nogo inhibitor of axon regeneration as a Reticulon protein. *Nature* **403**, 439–444 (2000).
- Prinjha, R. *et al.* Inhibitor of neurite outgrowth in humans. *Nature* **403**, 383–384 (2000).
- Tessier-Lavigne, M. & Goodman, C. S. Perspectives: neurobiology. Regeneration in the Nogo zone. *Science* **287**, 813–814 (2000).
- Fournier, A. E., GrandPre, T. & Strittmatter, S. M. Identification of a receptor mediating Nogo-66 inhibition of axonal regeneration. *Nature* **409**, 341–346 (2001).
- Luo, Y., Raible, D. & Raper, J. A. Collapsin: a protein in brain that induces the collapse and paralysis of neuronal growth cones. *Cell* **75**, 217–227 (1993).
- Mikol, D. D. & Stefansson, K. A phosphatidylinositol-linked peanut agglutinin-binding glycoprotein in central nervous system myelin and on oligodendrocytes. *J. Cell Biol.* **106**, 1273–1279 (1988).
- Mikol, D. D., Gulcher, J. R. & Stefansson, K. The oligodendrocyte-myelin glycoprotein belongs to a distinct family of proteins and contains the HNK-1 carbohydrate. *J. Cell Biol.* **110**, 471–479 (1990).
- He, Z. & Tessier-Lavigne, M. Neuropilin is a receptor for the axonal chemorepellent Semaphorin III. *Cell* **90**, 739–751 (1997).
- Habib, A. A. *et al.* Expression of the oligodendrocyte-myelin glycoprotein by neurons in the mouse central nervous system. *J. Neurochem.* **70**, 1704–1711 (1998).
- Niederost, B. P., Zimmermann, D. R., Schwab, M. E. & Bandtlow, C. E. Bovine CNS myelin contains neurite growth-inhibitory activity associated with chondroitin sulfate proteoglycans. *J. Neurosci.* **19**, 8979–8989 (1999).
- Spillmann, A. A., Bandtlow, C. E., Lottspeich, F., Keller, F. & Schwab, M. E. Identification and characterization of a bovine neurite growth inhibitor (bNI-220). *J. Biol. Chem.* **273**, 19283–19293 (1998).
- Flanagan, J. G. & Cheng, H. J. Alkaline phosphatase fusion proteins for molecular characterization and cloning of receptors and their ligands. *Methods Enzymol.* **327**, 198–210 (2000).
- Liu, B. P. & Strittmatter, S. M. Semaphorin-mediated axonal guidance via Rho-related G proteins. *Curr. Opin. Cell Biol.* **13**, 619–626 (2001).
- Norton, W. T. & Poduslo, S. E. Myelination in rat brain: method of myelin isolation. *J. Neurochem.* **21**, 749–757 (1973).
- Neve, R. L., Howe, J. R., Hong, S. & Kalb, R. G. Introduction of the glutamate receptor subunit 1 into motor neurons *in vitro* and *in vivo* using recombinant herpes simplex virus. *Neuroscience* **79**, 435–447 (1997).
- Huang, D. W., McKerracher, L., Braun, P. E. & David, S. A therapeutic vaccine approach to stimulate axon regeneration in the adult mammalian spinal cord. *Neuron* **24**, 639–647 (1999).
- Takahashi, T., Nakamura, F., Jin, Z., Kalb, R. G. & Strittmatter, S. M. Semaphorins A and E act as antagonists of neuropilin-1 and agonists of neuropilin-2 receptors. *Nature Neurosci.* **1**, 487–493 (1998).
- Cohen-Cory, S. & Fraser, S. E. Effects of brain-derived neurotrophic factor on optic axon branching and remodeling *in vivo*. *Nature* **378**, 192–196 (1995).

Supplementary Information accompanies the paper on Nature's website (<http://www.nature.com/nature>).

### Acknowledgements

We thank A. Habib and J. Flanagan for providing the anti-OMgp antibodies and the AP-5 plasmid, and M. Greenberg, X. He, D. Lowenstein and M. Tessier-Lavigne for reading the manuscript. This study was supported by the Alfred Sloan Foundation, the Burroughs Wellcome Fund, the EJLB Foundation, the International Spinal Research Trust, the John Merck Fund, the Klingenstein Fund, the Whitehall Foundation, and the National Institutes of Health (NIH). K.C.W. is a recipient of a Howard Hughes Predoctoral Fellowship. V.K. is supported by an NIH predoctoral training grant.

### Competing interests statement

The authors declare that they have no competing financial interests.

Correspondence and requests for materials should be addressed to Z.H. (e-mail: zhang.he@tch.harvard.edu).